HHS Public Access

Author manuscript

Doc Ophthalmol. Author manuscript; available in PMC 2019 February 01.

Published in final edited form as:

Doc Ophthalmol. 2018 February ; 136(1): 45–55. doi:10.1007/s10633-017-9620-z.

Electroretinography in idiopathic intracranial hypertension: comparison of the pattern ERG and the photopic negative response

Jason C. Park[a], **Heather E. Moss**[b,c], and **J. Jason McAnany**[a,d,*]

[a]Department of Ophthalmology and Visual Sciences, University of Illinois at Chicago, 1855 W. Taylor St., Chicago, IL 60612, USA

[b]Department of Ophthalmology, Stanford University, 2452 Watson Court, Palo Alto, CA, 94303

[c]Department of Neurology and Neuroscience, Stanford University, 2452 Watson Court, Palo Alto, CA 93403

[d]Department of Bioengineering, University of Illinois at Chicago, 851 South Morgan St., Chicago, IL 60607 USA

Abstract

Purpose—To evaluate the relationship between electrophysiological measures of retinal ganglion cell (RGC) function in patients who have idiopathic intracranial hypertension (IIH).

Methods—The pattern electroretinogram (pERG) and photopic negative response (PhNR) were recorded from 11 IIH patients and 11 age-similar controls. The pERG was elicited by a contrast reversing checkerboard. The PhNR, a slow negative component following the flash ERG b-wave, was recorded in response to a long-wavelength flash presented against a short-wavelength adapting field. The PhNR was elicited using full-field (ffPhNR) and focal macular (fPhNR) stimuli. Additionally, Humphrey visual field mean deviation (HVF MD) was measured and ganglion cell complex volume (GCCV) was obtained by optical coherence tomography.

Results—The ffPhNR, fPhNR and pERG amplitudes were outside of the normal range in 45%, 9%, and 45% of IIH patients, respectively. However, only mean ffPhNR amplitude was reduced significantly in the patients compared to controls ($p < 0.01$). The pERG amplitude correlated significantly with HVF MD and GCCV (both $r > 0.65$, $p < 0.05$). There were associations between ffPhNR amplitude and HVF MD ($r = 0.58$, $p = 0.06$) and with GCCV ($r = 0.52$, $p = 0.10$), but

*Corresponding author: J. Jason McAnany, Tel.: +1-312-355-3632., jmcana1@uic.edu.

Conflict of Interest: All authors certify that they have no affiliations with or involvement in any organization or entity with any financial interest (such as honoraria; educational grants; participation in speakers' bureaus; membership, employment, consultancies, stock ownership, or other equity interest; and expert testimony or patent-licensing arrangements), or non-financial interest (such as personal or professional relationships, affiliations, knowledge or beliefs) in the subject matter or materials discussed in this manuscript.

Ethical approval: All procedures performed in studies involving human participants were in accordance with the ethical standards of the institutional and/or national research committee and with the 1964 Helsinki declaration and its later amendments or comparable ethical standards.

Informed consent: Informed consent was obtained from all individual participants included in the study

these did not reach statistical significance. fPhNR amplitude was not correlated significantly with HVF MD or GCCV (both $r < 0.40$, $p > 0.20$).

Conclusions—Although the fPhNR is generally normal in IIH, other electrophysiological measures of RGC function, the ffPhNR and pERG, are abnormal in some patients. These measures provide complementary information regarding RGC dysfunction in these individuals.

Keywords

electroretinogram; pattern electroretinogram; photopic negative response; idiopathic intracranial hypertension

INTRODUCTION

Idiopathic intracranial hypertension (IIH) is a condition of elevated intracranial pressure (ICP) in individuals who do not have apparent abnormalities in brain structure or cerebrospinal fluid (CSF) [1]. Chronic papilledema, a significant consequence of elevated ICP, can lead to vision loss, with approximately 10% of IIH patients progressing to permanent bilateral blindness [1–3]. The events resulting in vision loss due to elevated ICP are reviewed elsewhere [4]. In brief, elevated ICP is thought to compress retinal ganglion cell (RGC) axons of the distal optic nerve and their blood supply, which leads to abnormalities in axoplasmic transport, intra-axonal edema, and dysfunction of RGCs, manifesting as vision loss in approximately 50% of cases [5–8]. Because vision loss is reversible in some individuals, careful assessment and monitoring is critical. In most clinical settings, standard automated perimetry (SAP) is used to evaluate peripheral visual field sensitivity, as the early effects of IIH are typically localized to the peripheral visual field [1,8–10]. However, SAP is an inherently subjective test and it may not have the necessary sensitivity to detect early manifestations of RGC injury [11].

Our group has focused on objective tests of inner-retina function in IIH, demonstrating varying degrees of abnormalities in pupillometry [12] and of the photopic negative response (PhNR) of full-field electroretinogram (ERG) [13]. The PhNR is a late negative component of the photopic single flash ERG that follows the b-wave. This response is most commonly elicited using a long-wavelength flash of light presented against short-wavelength adapting field. A series of studies in animal models [14,15] and in human patients with inner-retina diseases [16–20] are consistent with RGCs as the dominant source of the PhNR. The amplitude of the PhNR can be substantially decreased in IIH patients, and the loss of PhNR amplitude is correlated with standard clinical measures including Humphrey visual field mean deviation (HVF MD), Frisén papilledema grade (FPG), as well as with structural changes in RGC volume obtained by optical coherence tomography (OCT) [13].

In addition to PhNR measurement, other ERG techniques have been proposed to non-invasively assess post-receptor function including the pattern ERG (pERG) [21,22] and oscillatory potentials (OPs) [23]. The pERG is likely the most studied and best understood approach to studying RGC function [24] and international standards for measuring this response have been developed [25]. Contrast-reversing checkerboards and grating stimuli are commonly used to elicit the pERG. A previous study of the pERG in IIH patients, which

used grating stimuli, found pERG amplitude losses to be greatest for middle to high spatial frequencies (1.4 – 4.8 cycles/degree) [26]. A recent study using checkerboard stimuli showed small, but significant, losses in pERG amplitude for IIH patients using both moderate and small check sizes [27]. Similar to the PhNR findings, the loss of pERG amplitude was shown to correlate with OCT and visual field measures [27].

Although comparisons of the PhNR and pERG have been reported in visually-normal individuals [16,20], glaucoma patients [16,20,28,29], in a non-human primate model of glaucoma [30], and in autosomal dominant optic atrophy patients [31], the relationship between the PhNR and pERG has not been studies systematically in IIH patients. There is some reason to suspect that the PhNR and pERG may not provide identical measures of RGC function in IIH patients. That is, as typically measured, the PhNR is a full-field measure (ganzfeld stimulation) of RGC function that is sensitive to dysfunction of the peripheral retina, whereas the pERG is a macular test of RGC function (restricted area of stimulation). The location and size of the retinal area tested may be important in diseases such as IIH, where the initial site of dysfunction is typically localized to the periphery. Thus, the primary goal of the present study was to compare RGC deficits measured with the PhNR and pERG, and to determine how these responses relate to clinical tests of function (SAP) and structure (OCT). To better understand the effect of stimulus size on assessing RGC function, the PhNR was recorded using full-field (ffPhNR) and focal macular (fPhNR) stimuli that had a size equivalent to that of the pERG. The results of this study may be of use in guiding outcome measures in future treatment trials and for better understanding electrophysiological abnormalities in IIH patients.

METHODS

Subjects

Eleven subjects who have IIH and current or prior papilledema were recruited from the Neuro-ophthalmology service at the University of Illinois at Chicago (mean age 35.5 years; standard deviation 8.1 years, 10 females). Characteristics of the 11 subjects are provided in Table 1; subject 2 participated in a previous study of the PhNR in IIH [13]. The diagnosis of IIH was based on lumbar puncture with opening pressure ≥ 25 cm H_2O, normal cerebrospinal fluid constituents, and unremarkable brain imaging results [32]. No patient had neurological or ophthalmic disease other than IIH, refractive error greater than 6 diopters, or distance visual acuity worse than 20/20. The 24-2 HVF MD was considered normal (less than 2 dB loss) in 4 subjects, mildly abnormal (2 to 5 dB loss) in 3 subjects, and moderately to severely abnormal (more than 5 dB loss) in 4 subjects. Optic nerve appearance was evaluated and graded according to the Frisen papilledema grade (FPG) scale [33]: FPG was low (0, 1, 2) in 8 patients, high (3) in 1 patient, and 2 patients had optic atrophy. Data were also obtained from 11 visually-normal individuals (mean age 34.2 years; SD 6.1 years, 5 females) without history of ophthalmic or neurological disease. The mean ages of the controls and IIH subjects did not differ significantly ($t = 0.66$, $p = 0.52$).The research followed the tenets of the Declaration of Helsinki and was approved by a University of Illinois at Chicago institutional review board. Written informed consent was obtained from all subjects prior to testing.

Apparatus, stimuli, procedure

One eye from each subject was selected for testing. For the control subjects, the right eye was selected, whereas the eye with the worse HVF MD value was selected for the IIH patients. Stimuli for both the pERG and PhNR were generated using the Espion V6 electrophysiology console (Diagnosys, LLC). For the pERG, a checkerboard stimulus was displayed on a CRT monitor with refresh rate of 100 Hz (ViewSonic model G90FB). From the 57 cm test distance, each check subtended 0.9° and the total field size was 35° (width) × 25° (height). The photopic luminance of the light and dark checks was 82.4 cd/m^2 and 4.2 cd/m^2, respectively, yielding a Michelson contrast of 90%. The checkerboard contrast reversed at 2 Hz (4 reversals per second). Subjects viewed the checkerboard stimulus through appropriate refractive correction. ERGs were recorded with DTL fiber electrodes that were referenced to the ear (gold cup electrode); another gold cup electrode attached to the forehead served as the ground. At minimum of 150 sweeps that were free of blink artifacts were recorded and averaged for analysis for each subject. The pERG signals were recorded at a sampling rate of 2 kHz, with bandpass filter settings of 0.6 to 100 Hz.

Following the pERG recording, the pupil of the tested eye was dilated with 1% tropicamide and 2.5% phenylephrine hydrochloride drops. The PhNR was elicited using a long-wavelength pulse (dominant wavelength of 642 nm, 3 phot cd s m^2) presented against a short-wavelength adapting field (dominant wavelength of 465 nm, 12.5 phot cd m^2). The stimulus was either full field (ffPhNR) or focal (fPhNR). Focal stimulation was achieved by inserting a circular aperture (8 cm) between the opening of the ganzfeld dome and the subject's eye (description and photographs of the apparatus are presented elsewhere [34]). The viewing distance was 15 cm, which produced a field size of 32°. This size was selected to produce an area (804 deg^2) that was similar to that of the pERG area (875 deg^2). A minimum of five responses that were not contaminated by eye blink artifacts were obtained and averaged for analysis for each subject. The ffPhNR and fPhNR signals were recorded at a sampling rate of 2 kHz with bandpass filter settings of 0.3 to 300 Hz. As for the pERG recordings, the PhNR was recorded using DTL fiber electrodes, with the ear and forehead serving as reference and ground, respectively. Stimulus wavelength and luminance were verified with a spectroradiometer (SpectraScan® 740, Photo Research).

Ganglion cell complex volume (GCCV) was measured from 20° × 15° high-resolution macular scans obtained by OCT (Spectralis; Heidelberg Engineering, Inc.) using the Eye Explorer software provided by the manufacturer [35]. To calculate GCCV, the internal limiting membrane was defined based on the automated segmentation feature of the Heidelberg software. Next, the boundary between the inner plexiform layer and inner nuclear layer was defined by manual selection of key points to which a series of splines were automatically fit. GCCV was automatically calculated as the volume between these boundaries within a 3-mm cylindrical volume centered on the fovea.

Data analysis

For the pERG analysis, three amplitude measurements were derived from the waveform: 1) the first positive peak of the waveform (P50), the subsequent negative trough (N95), and the sum of the P50 and N95 components (P50 + N95). The P50 and N95 were selected using a

semi-automated, custom-made MATLAB script (MathWorks Inc). This semi-automated script also permitted selection of the a-wave, b-wave, and the PhNR from the full-field and focal single flash waveforms. The PhNR amplitude was defined as the difference between the mean baseline amplitude (10 ms before the stimulus was presented) and the mean amplitude within a 5 ms window centered at the trough of the response, consistent with a previous definition [13,36]. In accordance with a previous study, the PhNR amplitude was also normalized by the sum of the PhNR and b-wave amplitudes: PhNR / [PhNR + b-wave amplitude], which reduces variation among subjects due to overall response amplitude [36].

Results

Fig. 1 shows the ERG traces for each patient compared to the control range (gray region) for the ffPhNR (top), fPhNR (middle), and pERG (bottom). As expected, the waveform obtained under the ffPhNR condition, elicited by a full-field flash, is characterized by a- and b-waves, followed by a slow negative response (the PhNR). The trough of the ffPhNR occurred at approximately 70 ms for both the control subjects and IIH patients. Although 2 of the 11 patients had robust ffPhNRs, the other 9 patients were at the limit of normal, or were outside of the normal range. Fig. 1B shows that the fPhNR waveform, elicited by the 32° flash, is also characterized by a- and b-waves, followed by the PhNR. However, the a- and b-wave amplitudes were smaller and the trough of the fPhNR was delayed slightly relative to the ffPhNR (approximately 80 ms). The patients' fPhNRs were generally within the upper limit of the control range. The pERG waveforms were characterized by a small N35 component, followed by larger P50 and N95 components. The N35 and P50 response components were generally within the control range for the IIH patients. The N95 component for the patients ranged from normal (N=6) to attenuated (N=5). The traces shown in Fig. 1 are intended to illustrate the general pattern of responses; the ffPhNR, fPhNR and pERG amplitudes are examined quantitatively below.

Fig. 2 (top) shows the distribution of ffPhNR and fPhNR amplitudes for the patients (each patient is indicated by a symbol that corresponds to that given in Table 1) and control subjects (the gray region is the control range; control mean is indicated by the black horizontal bar). The right two data sets shown in Fig. 2 (top) represent the same data normalized to the b-wave, as discussed in the Methods; these data are plotted with respect to the right y-axis. For the ffPhNR amplitude (leftmost dataset), five IIH patients had amplitudes that fell outside of the normal range (45% of the sample). After normalizing by the b-wave amplitude, six patients (55%) were outside of the normal range (third dataset from the left). For the fPhNR, one patient fell slightly outside of the normal range (second dataset from the left); after normalization by the b-wave amplitude, one patient was outside of the normal range (rightmost dataset). The lower panel of Figure 2 shows the distribution of the P50, N95 and P50 + N95 amplitudes for the patients (symbols) and the controls (gray range). All patients had P50 amplitudes in the normal range, whereas 5 patients (45%) had N95 amplitudes that fell outside of the normal range. These 5 patients all had HVF MD losses of at least 3 dB. When the two components were combined (P50 + N95), two patients fell below the normal range (18%). The rightmost data set shows the normalized N95/P50 amplitude. Normalization had minimal effects on the pattern of data: the same 5 subjects who had N95 amplitude loss also had abnormally low N95/P50 ratios.

The amplitudes were analyzed statistically using a set of two-way repeated measures ANOVAs. ANOVA performed on the non-normalized PhNR data indicated a significant effect of field size (fPhNR vs ffPhNR; $F = 37.26$, $p < 0.001$) and group (control vs IIH; $F = 5.02$, $p = 0.04$). There was also a significant interaction between field size and group ($F = 8.88$, $p = 0.01$). Bonferroni-corrected pairwise comparisons indicated a significant difference between the patients and controls for the ffPhNR ($t = 3.31$, $p < 0.01$), but not the fPhNR ($F = 0.74$, $p = 0.47$). The results of the analyses were not changed materially after normalizing the PhNR by the b-wave. Reducing the field size resulted in a significant amplitude decrease for the control subjects (mean decrease of 42%; $t = 12.08$, $p < 0.001$), but not for the patients (mean decrease of 23%; $t = 1.86$, $p = 0.09$). ANOVA performed on the pERG data indicated a significant effect of waveform component (P50, N95, P50+N95; $F = 192.05$, $p < 0.001$), but not group (control vs IIH; $F = 0.18$, $p = 0.68$). There was no significant interaction between component and group ($F = 0.85$, $p = 0.44$) and there were no significant differences between the controls and patients for any pERG component (all $t < 0.75$, $p > 0.46$). Normalizing the N95 component by the P50 component did not meaningfully affect the results of the analysis: the mean normalized N95 did not differ significantly for the control and IIH subjects ($t = 0.77$, $p = 0.45$).

Table 2A shows the correlation matrix for the OCT, HVF MD, and ERG measurements for the IIH patients; amplitude was converted to log amplitude for comparison to the HVF MD (dB) values. Although there was an association between the log ffPhNR amplitude and HVF MD ($r = 0.58$, $p = 0.06$), as well as between the log fPhNR amplitude and HVF MD ($r = 0.40$, $p = 0.23$), the correlations were not statistically significant. Similarly, the correlation between both PhNR measures and GCCV did not reach statistical significance (both $r \leq 0.42$, $p \geq 0.20$). In comparison, the pERG N95 and N95+P50 parameters were correlated significantly with functional (HVF MD) and structural (GCCV) measures (all $r \geq 0.65$, $p \leq 0.03$). Table 2B shows the correlations for the ERG measurements performed in the control subjects. In contrast to the pattern observed for the IIH subjects, log ffPhNR amplitude was correlated significantly with log fPhNR amplitude for the controls ($r = 0.89$, $p < .001$.) There were also significant correlations between the pERG amplitudes and both PhNR measures, which were generally not observed for the IIH subjects.

Discussion

The present study evaluated RGC function in IIH patients using two established electrophysiological measures of inner-retina function, the PhNR and pERG, and compared these electrophysiological recordings to clinical tests of function (HVF MD) and structure (OCT). The results indicated significant differences in the mean full-field PhNR amplitude between the control and IIH subjects. Although individual subjects had marked pERG N95 amplitude reductions and the mean N95 amplitude was lower in IIH subjects compared to the control mean, the amplitude reduction did not meet the threshold for statistical significance. To better understand the effect of stimulus size on the RGC function measurements, the PhNR was recorded using a focal stimulus (fPhNR) that had a size approximately equivalent to that of the pERG. Reducing the PhNR field size reduced the differences in amplitude between the control and IIH groups, resulting in non-significant differences in fPhNR amplitude between the two groups.

The finding of statistically significant amplitude reductions for the IIH subjects for the ffPhNR, but not the fPhNR, can be likely attributed to the retinal area assessed with these stimuli. Specifically, early visual field loss in IIH localizes to the peripheral retina, with macular involvement not occurring until advanced stages of disease [1,8–10]. Full-field stimuli capture abnormalities throughout the retina, whereas focal stimuli target central retinal abnormalities. Thus, the difference between full-field and focal responses largely represents the response contributed by the peripheral retina. In this study, reducing the field size decreased the PhNR amplitude for the control subjects substantially, but had less effect for the IIH patients. This suggests that the peripheral retina contributed less to the ffPhNR amplitude for IIH subjects compared to the control subjects, which supports use of the ffPhNR as a marker of ganglion cell dysfunction in IIH. Of note, the two patients who had the largest ffPhNR amplitudes (patients 3 and 11) did show a clear amplitude reduction for the fPhNR, suggesting that the peripheral retina of these two patients had significant contributions to the ffPhNR.

The results of the present study differ somewhat from two previous reports [26,27], in that the mean pERG amplitude of the patients and controls did not differ significantly. Alfonso et al. [27] showed small, but statistically significant, amplitude differences between IIH patients and controls (e.g. 1.4 μV for the N95 component), which are slightly larger than those observed in the present study (e.g. 0.8 μV for the N95 component). Falsini et al [26], who measured the steady-state pERG, showed amplitude reductions in 77% of their patients. The statistically non-significant differences in pERG amplitudes in the present study may be due to our relatively small sample size (11 eyes of 11 patients), compared to the previous studies (38 eyes of 24 patients in [27] and 18 patients in [26]). Additionally, the steady-state pERG measurement performed previously [26] may have lower variability and a higher signal-to-noise ratio compared to the transient pERG used here. In future work, it would be of interest to compare steady-state and transient pERGs in patients who have IIH. Nevertheless, in the present study, the amplitude reductions in patients who had pERG abnormalities were most apparent in the N95 component (5 of the 11 IIH patients were abnormal). In contrast, all of our subjects had a P50 component in the range of normal. This finding is consistent with previous data indicating that the P50 and N95 components may have different sources. Specifically, the N95 component of the pERG is thought to arise mainly from RGCs, whereas the P50 is likely generated by a combination of RGCs and contributions from sources distal to the RGCs [37]. In this context, the selective N95 deficits in our IIH patients suggest a site of dysfunction that is specific to the RGCs.

As indicated above, there was a trend for the pERG N95 to be reduced for the IIH patients (5 of the 11 IIH patients were abnormal), but this trend was not apparent for the fPhNR (only one patient was slightly outside of the normal range), despite the similar areas that these stimuli subtended. This difference is consistent with previous work showing that the pERG can be abnormal in areas of the visual field that have normal perimetric sensitivity [38–42]. By contrast, PhNR abnormalities appear to be localized to the area of the field defect [16,43]. This suggests that the PhNR may sample the local activity of the area stimulated, whereas the pERG may pool responses from a broader area (a “panretinal” response [16,38]). Of note, the poor ability of the fPhNR to identify abnormalities in IIH is not consistent with the good sensitivity and specificity of the fPhNR for identifying

abnormalities in early to intermediate stage glaucoma patients [44]. However, the pathophysiology of glaucoma and IIH differ substantially, so findings in glaucoma do not necessarily translate directly to IIH. It is also possible that the macula is more affected in glaucoma than IIH, which could account for the fPhNR differences between IIH and glaucoma.

Consistent with previous work [27], the pERG N95 and pERG P50+N95 amplitudes were correlated significantly with other functional and structural measures. The P50 amplitude, however, was not correlated significantly with HVF MD or GCCV in the present study. Log ffPhNR amplitude was associated with HVF MD and GCCV, but the correlations did not reach statistical significance ($p = 0.06$ and $p = 0.10$ for HVF MD and GCCV, respectively). The borderline non-significant values are likely due to the sample size and the relatively mild disease severity of most patients in the present study; combining the present data set with that published previously [13] resulted in stronger, statistically significant correlations between log ffPhNR amplitude and HVF MD ($r = 0.64$, $p < 0.01$, $N = 20$), as well as between log ffPhNR amplitude and GCCV ($r = 0.48$, $p = 0.03$, $N = 20$).

Log fPhNR amplitude was also not correlated significantly with HVF MD or GCCV. The IIH subjects had a wide range of HVF MD values (−1 to −30 dB), but their fPhNR amplitudes were generally within the range of normal. Although the two IIH subjects with the greatest HVF MD loss also had relatively small fPhNR amplitudes, three of the four IIH subjects who had normal HVF MD values had fPhNR amplitudes at or below the normal mean. In general, the fPhNR does not appear to be a particularly useful index of RGC function in IIH patients. That is, it is not reduced significantly in these individuals and it does not correlate well with other structural and functional measures. In contrast, the pERG measures do correlate well with other structural and functional measures, suggesting that the pERG may be a more useful index of macular RGC function. The explanation for the differences between the pERG and fPhNR are not entirely clear, but these two tests of macular RGC function differ in several respects including adaptation level, stimulus type (i.e. achromatic pattern vs chromatic diffuse), as well as stimulus duration and luminance. It is also possible that the PhNR and pERG measures are biased toward different sub-types of RGCs, which could affect their associations with other clinical measures. This possibility is consistent with the local versus pan-retinal distinction between these measures noted above; future work is needed to evaluate this further.

In summary, the results indicate that electrophysiological measures of RGC function, the PhNR and pERG, provide complementary information regarding RGC dysfunction in IIH patients. The pERG is useful in that it provides information regarding macular RGC abnormalities, and the amplitude of the response correlates with both structural and functional measures. Although the correlation between the ffPhNR and structural and functional measures is somewhat weaker, the ffPhNR can capture RGC dysfunction that is confined to, or predominately in, the peripheral retina.

Acknowledgments

Supported by the National Institutes of Health Grants K12EY021475 (HM), K23EY024345 (HM), and P30EY01792 (UIC Core); an Illinois Society for the Prevention of Blindness Research Grant (HM); an unrestricted

departmental grant, Sybil B. Harrington (HM) and Dolly Green (JM) Special Scholar Awards from Research to Prevent Blindness.

Funding: The National Institutes of Health, Research to Prevent Blindness, and the Illinois Society for the Prevention of Blindness provided financial support in the form of funding. The sponsors had no role in the design or conduct of this research.

References

1. Wall M. Idiopathic intracranial hypertension. Neurol Clin. 1991; 9(1):73–95. [PubMed: 2011112]
2. Corbett JJ, Savino PJ, Thompson HS, Kansu T, Schatz NJ, Orr LS, Hopson D. Visual loss in pseudotumor cerebri. Follow-up of 57 patients from five to 41 years and a profile of 14 patients with permanent severe visual loss. Arch Neurol. 1982; 39(8):461–474. [PubMed: 7103794]
3. Orcutt JC, Page NG, Sanders MD. Factors affecting visual loss in benign intracranial hypertension. Ophthalmology. 1984; 91(11):1303–1312. [PubMed: 6514295]
4. Lee AG, Wall M. Papilledema: are we any nearer to a consensus on pathogenesis and treatment? Curr Neurol Neurosci Rep. 2012; 12(3):334–339. DOI: 10.1007/s11910-012-0257-8 [PubMed: 22354546]
5. Hayreh SS. Pathogenesis of optic disc oedema in raised intracranial pressure. Trans Ophthalmol Soc U K. 1976; 96(3):404–407. [PubMed: 829180]
6. Hayreh SS. Optic disc edema in raised intracranial pressure. V. Pathogenesis. Arch Ophthalmol. 1977; 95(9):1553–1565. [PubMed: 71138]
7. Hayreh SS, March W, Anderson DR. Pathogenesis of block of rapid orthograde axonal transport by elevated intraocular pressure. Exp Eye Res. 1979; 28(5):515–523. [PubMed: 87337]
8. Tso MO, Hayreh SS. Optic disc edema in raised intracranial pressure. IV. Axoplasmic transport in experimental papilledema. Arch Ophthalmol. 1977; 95(8):1458–1462. [PubMed: 70201]
9. Rowe FJ, Sarkies NJ. Assessment of visual function in idiopathic intracranial hypertension: a prospective study. Eye (Lond). 1998; 12(Pt 1):111–118. DOI: 10.1038/eye.1998.18 [PubMed: 9614526]
10. Wall M, George D. Visual loss in pseudotumor cerebri. Incidence and defects related to visual field strategy. Arch Neurol. 1987; 44(2):170–175. [PubMed: 3813933]
11. Calkins DJ. Critical pathogenic events underlying progression of neurodegeneration in glaucoma. Prog Retin Eye Res. 2012; 31(6):702–719. DOI: 10.1016/j.preteyeres.2012.07.001 [PubMed: 22871543]
12. Park JC, Moss HE, McAnany JJ. The Pupillary Light Reflex in Idiopathic Intracranial Hypertension. Invest Ophthalmol Vis Sci. 2016; 57(1):23–29. DOI: 10.1167/iovs.15-18181 [PubMed: 26746015]
13. Moss HE, Park JC, McAnany JJ. The Photopic Negative Response in Idiopathic Intracranial Hypertension. Invest Ophthalmol Vis Sci. 2015; 56(6):3709–3714. DOI: 10.1167/iovs.15-16586 [PubMed: 26047172]
14. Viswanathan S, Frishman LJ, Robson JG, Harwerth RS, Smith EL 3rd. The photopic negative response of the macaque electroretinogram: reduction by experimental glaucoma. Invest Ophthalmol Vis Sci. 1999; 40(6):1124–1136. [PubMed: 10235545]
15. Rangaswamy NV, Shirato S, Kaneko M, Digby BI, Robson JG, Frishman LJ. Effects of spectral characteristics of ganzfeld stimuli on the photopic negative response (PhNR) of the ERG. Invest Ophthalmol Vis Sci. 2007; 48(10):4818–4828. DOI: 10.1167/iovs.07-0218 [PubMed: 17898309]
16. Preiser D, Lagreze WA, Bach M, Poloschek CM. Photopic negative response versus pattern electroretinogram in early glaucoma. Invest Ophthalmol Vis Sci. 2013; 54(2):1182–1191. DOI: 10.1167/iovs.12-11201 [PubMed: 23307968]
17. Viswanathan S, Frishman LJ, Robson JG, Walters JW. The photopic negative response of the flash electroretinogram in primary open angle glaucoma. Invest Ophthalmol Vis Sci. 2001; 42(2):514–522. [PubMed: 11157891]
18. Wang J, Cheng H, Hu YS, Tang RA, Frishman LJ. The photopic negative response of the flash electroretinogram in multiple sclerosis. Invest Ophthalmol Vis Sci. 2012; 53(3):1315–1323. DOI: 10.1167/iovs.11-8461 [PubMed: 22273726]

19. Nakamura H, Miyamoto K, Yokota S, Ogino K, Yoshimura N. Focal macular photopic negative response in patients with optic neuritis. Eye (Lond). 2011; 25(3):358–364. DOI: 10.1038/eye.2010.205 [PubMed: 21212800]
20. Sustar M, Cvenkel B, Brecelj J. The effect of broadband and monochromatic stimuli on the photopic negative response of the electroretinogram in normal subjects and in open-angle glaucoma patients. Doc Ophthalmol. 2009; 118(3):167–177. DOI: 10.1007/s10633-008-9150-9 [PubMed: 18932006]
21. Mafei L, Fiorentini A. Electroretinographic responses to alternating gratings before and after section of the optic nerve. Science. 1981; 211(4485):953–955. [PubMed: 7466369]
22. Porciatti V, Saleh M, Nagaraju M. The pattern electroretinogram as a tool to monitor progressive retinal ganglion cell dysfunction in the DBA/2J mouse model of glaucoma. Invest Ophthalmol Vis Sci. 2007; 48(2):745–751. DOI: 10.1167/iovs.06-0733 [PubMed: 17251473]
23. Wachtmeister L. Oscillatory potentials in the retina: what do they reveal. Prog Retin Eye Res. 1998; 17(4):485–521. [PubMed: 9777648]
24. Porciatti V. Electrophysiological assessment of retinal ganglion cell function. Exp Eye Res. 2015; 141:164–170. DOI: 10.1016/j.exer.2015.05.008 [PubMed: 25998495]
25. Bach M, Brigell MG, Hawlina M, Holder GE, Johnson MA, McCulloch DL, Meigen T, Viswanathan S. ISCEV standard for clinical pattern electroretinography (PERG): 2012 update. Doc Ophthalmol. 2013; 126(1):1–7. DOI: 10.1007/s10633-012-9353-y [PubMed: 23073702]
26. Falsini B, Tamburrelli C, Porciatti V, Anile C, Porrello G, Mangiola N. Pattern electroretinograms and visual evoked potentials in idiopathic intracranial hypertension. Ophthalmologica. 1992; 205(4):194–203. [PubMed: 1484689]
27. Afonso CL, Raza AS, Kreuz AC, Hokazono K, Cunha LP, Oyamada MK, Monteiro ML. Relationship Between Pattern Electroretinogram, Frequency-Domain OCT, and Automated Perimetry in Chronic Papilledema From Pseudotumor Cerebri Syndrome. Invest Ophthalmol Vis Sci. 2015; 56(6):3656–3665. DOI: 10.1167/iovs.15-16768 [PubMed: 26047166]
28. Drasdo N, Aldebasi YH, Chiti Z, Mortlock KE, Morgan JE, North RV. The s-cone PHNR and pattern ERG in primary open angle glaucoma. Invest Ophthalmol Vis Sci. 2001; 42(6):1266–1272. [PubMed: 11328738]
29. North RV, Jones AL, Drasdo N, Wild JM, Morgan JE. Electrophysiological evidence of early functional damage in glaucoma and ocular hypertension. Invest Ophthalmol Vis Sci. 2010; 51(2):1216–1222. DOI: 10.1167/iovs.09-3409 [PubMed: 19850843]
30. Wilsey L, Gowrisankaran S, Cull G, Hardin C, Burgoyne CF, Fortune B. Comparing three different modes of electroretinography in experimental glaucoma: diagnostic performance and correlation to structure. Doc Ophthalmol. 2017; 134(2):111–128. DOI: 10.1007/s10633-017-9578-x [PubMed: 28243926]
31. Morny EK, Margrain TH, Binns AM, Votruba M. Electrophysiological ON and OFF Responses in Autosomal Dominant Optic Atrophy. Invest Ophthalmol Vis Sci. 2015; 56(13):7629–7637. DOI: 10.1167/iovs.15-17951 [PubMed: 26624494]
32. Friedman DI, Jacobson DM. Diagnostic criteria for idiopathic intracranial hypertension. Neurology. 2002; 59(10):1492–1495. [PubMed: 12455560]
33. Frisen L. Swelling of the optic nerve head: a staging scheme. J Neurol Neurosurg Psychiatry. 1982; 45(1):13–18. [PubMed: 7062066]
34. Park JC, McAnany JJ. Effect of stimulus size and luminance on the rod-, cone-, and melanopsin-mediated pupillary light reflex. J Vis. 2015; 15(3):13.doi: 10.1167/15.3.13
35. Krebs I, Smretschnig E, Moussa S, Brannath W, Womastek I, Binder S. Quality and reproducibility of retinal thickness measurements in two spectral-domain optical coherence tomography machines. Invest Ophthalmol Vis Sci. 2011; 52(9):6925–6933. DOI: 10.1167/iovs.10-6612 [PubMed: 21791591]
36. Kundra H, Park JC, McAnany JJ. Comparison of photopic negative response measurements in the time and time-frequency domains. Doc Ophthalmol. 2016; 133(2):91–98. DOI: 10.1007/s10633-016-9558-6 [PubMed: 27562839]
37. Holder GE. Pattern electroretinography (PERG) and an integrated approach to visual pathway diagnosis. Prog Retin Eye Res. 2001; 20(4):531–561. [PubMed: 11390258]

38. Bach M, Hoffmann MB. Update on the pattern electroretinogram in glaucoma. Optom Vis Sci. 2008; 85(6):386–395. DOI: 10.1097/OPX.0b013e318177ebf3 [PubMed: 18521020]

39. Bach M, Pfeiffer N, Birkner-Binder D. Pattern-Electroretinogram reflects diffuse retinal damage in early glaucoma. Clin Vision Sci. 1992; 7(4):335–340.

40. Bach M, Sulimma F, Gerling J. Little correlation of the pattern electroretinogram (PERG) and visual field measures in early glaucoma. Doc Ophthalmol. 1997; 94(3):253–263. [PubMed: 9682994]

41. Harrison WW, Viswanathan S, Malinovsky VE. Multifocal pattern electroretinogram: cellular origins and clinical implications. Optom Vis Sci. 2006; 83(7):473–485. DOI: 10.1097/01.opx.0000218319.61580.a5 [PubMed: 16840872]

42. Klistorner AI, Graham SL, Martins A. Multifocal pattern electroretinogram does not demonstrate localised field defects in glaucoma. Doc Ophthalmol. 2000; 100(2–3):155–165. [PubMed: 11142744]

43. Machida S. Clinical applications of the photopic negative response to optic nerve and retinal diseases. J Ophthalmol. 2012; 2012:397178.doi: 10.1155/2012/397178 [PubMed: 23133741]

44. Machida S, Tamada K, Oikawa T, Gotoh Y, Nishimura T, Kaneko M, Kurosaka D. Comparison of photopic negative response of full-field and focal electroretinograms in detecting glaucomatous eyes. J Ophthalmol. 2011; 2011doi: 10.1155/2011/564131

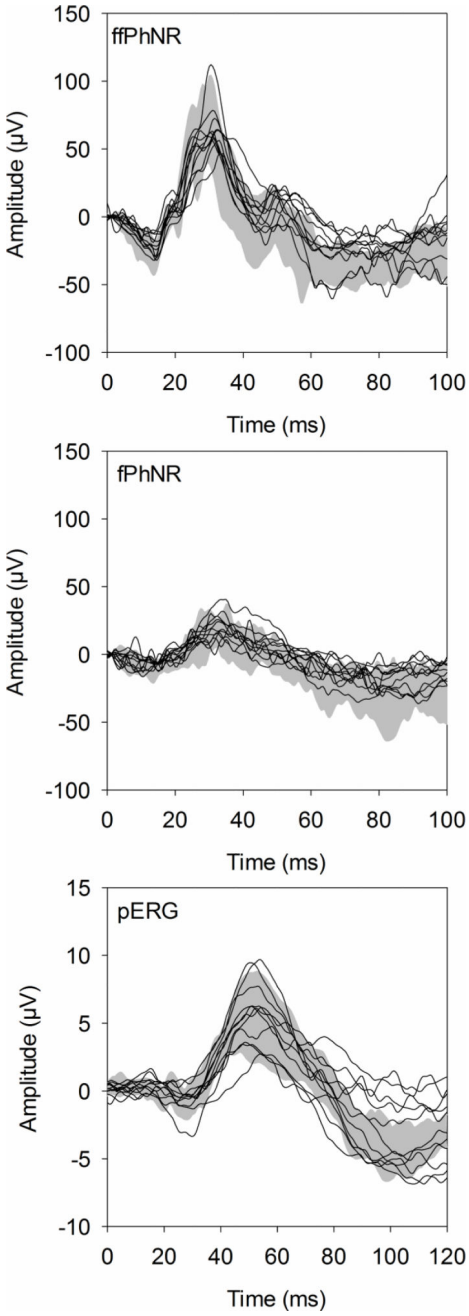

Figure 1.

Waveforms obtained for the ffPhNR (top), fPhNR (middle), and pERG (bottom). Each trace represents a response from an IIH subject and the gray region represents the range of responses from the visually-normal subjects.

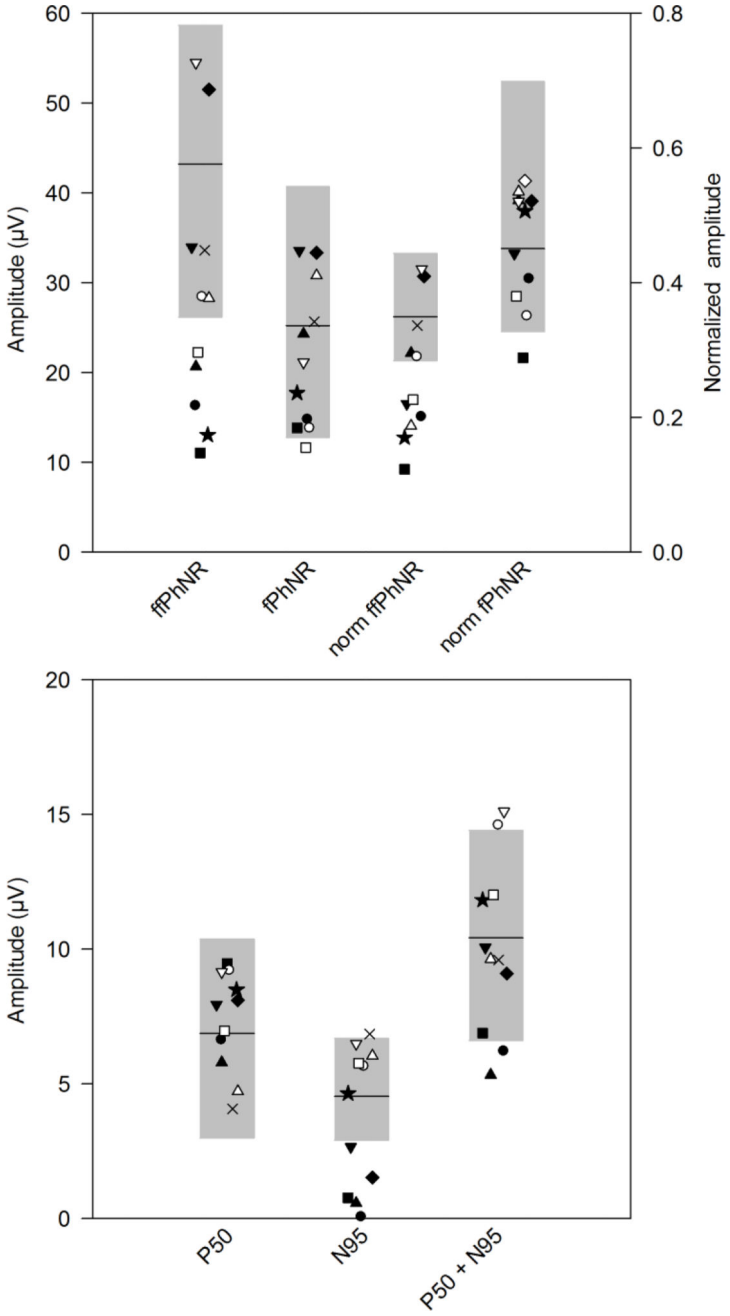

Figure 2.

Distribution of amplitudes. Amplitudes for each IIH subject are represented by the symbols (corresponding to those given in Table 1) and the gray regions represent the range of amplitudes obtained from the visually-normal subjects; horizontal black bars indicate the normal mean. In the top panel, data are shown for the ffPhNR (1st data set) and the fPhNR (2nd data set). The 3rd and 4th data sets represent the b-wave normalized ffPhNR and fPhNR, respectively. The normalized data are plotted with respect to the right y-axis. The lower

panel shows amplitudes for the pERG P50, N95, and P50+N95 amplitudes, respectively. The normalized N95/P50 amplitude is plotted with respect to the right y-axis.

Table 1

Idiopathic intracranial hypertension subject characteristics

ID	Eye	Age (yrs)	Sex	FPG	GCCV (mm^3)	HVF MD (dB)
1 ●	OD	26	F	Atrophy	0.36	−31.74
2 ■	OS	35	F	Atrophy	0.42	−26.43
3 ◆	OD	37	F	1	0.71	−6.48
4 ▲	OD	30	F	1	0.62	−5.84
5 ▼	OD	27	M	3	0.88	−3.14
6 ★	OD	46	F	0	0.77	−2.98
7 ○	OD	27	F	2	0.70	−2.53
8 □	OD	38	F	1	0.72	−1.92
9 ×	OD	37	F	1	0.74	−1.83
10 △	OD	52	F	0	0.75	−1.63
11 ▽	OS	36	F	2	0.79	−1.12

OD = right eye, OS = left eye, F=female, M=male

Table 2

A: IIH correlation matrix for ERG, HVF-MD, and OCT measures						
	GCCV	**HVF-MD**	**ffPhNR (log μV)**	**fPhNR (log μV)**	**P50 (log μV)**	**N95 (log μV)**
HVF-MD	**0.964 (p < 0.001)**					
ffPhNR (log μV)	0.521 (p = 0.100)	0.579 (p = 0.062)				
fPhNR (log μV)	0.421 (p = 0.197)	0.397 (p = 0.226)	0.595 (p = 0.054)			
P50 (log μV)	−0.069 (p = 0.841)	−0.179 (p = 0.599)	−0.093 (p = 0.786)	−0.374 (p = 0.257)		
N95 (log μV)	**0.871 (p < .001)**	**0.870 (p < 0.001)**	0.427 (p = 0.191)	0.173 (p = 0.612)	−0.047 (p = 0.891)	
N95+P50 (log μV)	**0.693 (p = 0.018)**	**0.645 (p = 0.032)**	0.457 (p = 0.157)	−0.105 (p = 0.758)	0.325 (p = 0.330)	**0.797 (p = 0.003)**

B: Control correlation matrix for ERG measures				
	ffPhNR (log μV)	**fPhNR (log μV)**	**P50 (log μV)**	**N95 (log μV)**
fPhNR (log μV)	**0.893 (p < 0.001)**			
P50 (log μV)	**0.801 (p = 0.003)**	**0.657 (p = 0.028)**		
N95 (log μV)	0.519 (p = 0.102)	**0.610 (p = 0.046)**	0.557 (p = 0.075)	
N95+P50 (log μV)	**0.856 (p < 0.001)**	**0.832 (p = 0.001)**	**0.910 (p < 0.001)**	**0.801 (p = 0.003)**